Expression levels of hnRNP K and p21[WAF1/CIP1] are associated with resistance to radiochemotherapy independent of p53 pathway activation in rectal adenocarcinoma

WASSILIKI DASKALAKI[1], EVA WARDELMANN[1], MATTHIAS PORT[2], KATHARINA STOCK[1],
JULIE STEINESTEL[3], SEBASTIAN HUSS[1], JAN SPERVESLAGE[1],
KONRAD STEINESTEL[1,4*] and STEFAN EDER[2*]

[1]Gerhard-Domagk-Institute of Pathology, University Hospital Münster, D-48149 Münster;
[2]Bundeswehr Institute of Radiobiology Affiliated to The University of Ulm, D-80937 Munich;
[3]Department of Urology, University Hospital Münster, D-48149 Münster;
[4]Institute of Pathology and Molecular Pathology, Bundeswehrkrankenhaus, D-89081 Ulm, Germany

Abstract. Ionizing radiation (IR) is frequently applied in the treatment of rectal adenocarcinoma, however, there is marked variance in the response to radiochemotherapy between individual tumors. In our previous investigations, it was shown that the overexpression of heterogeneous nuclear ribonucleoprotein K (hnRNP K) confers radioresistance to malignant melanoma and colorectal carcinoma (CRC) *in vitro*, however, the underlying mechanism remains to be elucidated. As hnRNP K, a p53 binding partner and cofactor for the transcriptional activation of p53 target genes, is overexpressed in CRC, the present study investigated the possible radioprotective effect of the hnRNP K/p53-induced upregulation of p21 (also known as WAF1/CIP1) in rectal adenocarcinoma. Immunohistochemistry was performed for hnRNP K, p53 and p21 in a series of 68 consecutive cases of rectal adenocarcinoma with full molecular characterization following radiochemotherapy and 14 corresponding pre-therapeutic biopsies, and the results were correlated with clinicopathological characteristics and the percentage of vital tumor cells following therapy. In addition, pathway analyses, protein immunoprecipitation, western immunoblotting and immunofluorescence microscopy were performed to identify dysregulated kinase signaling and hnRNP K targets upon exposure of CRC cells to IR. Although the fraction of vital tumor cells upon neoadjuvant therapy was significantly higher in hnRNP K/p21-positive tumors (P=0.0047 and P=0.0223, Students' t-test), no significant association was found between the protein expression levels of hnRNP K, p53 and p21 (P>0.05, χ^2 test). Irradiation enhanced apoptotic pathway activation via p53/CHK2 phosphorylation and poly (ADP-ribose) polymerase cleavage, and induced the overexpression and interaction of hnRNP K and p53. However, p53 Ser15-phosphorylation was independent of the presence of hnRNP K, and there was no measurable effect of hnRNP K on the expression of p21 *in vitro*. Taken together, the results of the present study support a radioprotective role for hnRNP K, which may be mediated through an interaction with p53, however, this effect appears to be independent of the hnRNP K/p53-induced upregulation of p21 in rectal adenocarcinoma.

Introduction

Colorectal cancer (CRC) is one of the most common types of cancer and is the third leading cause of cancer-associated mortality in men and women in the western world (1). Rectal adenocarcinoma comprises up to 30% of these tumors and they are frequently treated with (neoadjuvant) radiochemotherapy (RCTx) to reduce tumor mass prior to surgery (2,3). It has been shown that short-term preoperative RCTx reduces the risk of local recurrence, overall mortality rate and cancer-associated mortality rate in patients who undergo a standardized total mesorectal excision (3,4). In Germany, pre-operative radiation therapy comprises short-term (5x5 Gy on 5 subsequent days) and long-term radiation protocols (fractionated scheme of 2 Gy/week to a cumulative dose of 45-50.4 Gy) (5). However, not all types of rectal carcinoma respond to RCTx equally. Although 15-27% of patients show pathological complete response (pCR, no remaining vital tumor cells) associated with an improved long-term outcome, a significant proportion of tumors exhibit variable degrees of therapy resistance (6). This

Correspondence to: Dr Konrad Steinestel, Institute of Pathology and Molecular Pathology, Bundeswehrkrankenhaus Ulm, 40 Oberer Eselsberg, D-89081 Ulm, Germany
E-mail: konrad@steinestel.com

*Contributed equally

issue has been addressed by pathologists with the introduction of classification schemes that describe the degree of tumor regression in response to neoadjuvant therapy (7-9). However, biomarkers that can reliably predict sensitivity of an individual tumor to neoadjuvant RCTx have not been identified.

Heterogeneous nuclear ribonucleoprotein K (hnRNP K) is a ubiquitously expressed 65 kDa-protein containing three eponymous K homology domains that mediate binding to poly(C) regions in DNA and RNA to regulate gene transcription, pre-mRNA maturation processes and translation (10,11). HnRNP K is upregulated and associated with poor prognosis in multiple malignancies, including CRC, and it has been shown in previous studies that hnRNP K confers radioresistance to CRC and malignant melanoma cells in a mitogen-activated protein kinase (MAPK)-dependent manner (12-15). At present, whether hnRNP K represents a valuable biomarker for radioresistance and, in particular, how the downstream effects of hnRNP K protect the tumor cells from the deleterious effects of ionizing radiation (IR) remain to be elucidated. It is known that hnRNP K acts as a transcriptional cofactor in the induction of p53 target genes following DNA damage upon protein/protein interaction with p53, leading to the upregulation of p21 (also known as WAF1/CIP1; Fig. 1) (16-19). By contrast, p21 acts as a cyclin-dependent kinase inhibitor and is an important component of the G_1 checkpoint response to DNA damage (20).

Therefore, the aim of the present study was to investigate whether the expression of hnRNP K is associated with poor response to RCTx in rectal cancer, and also whether a possible radioprotective effect is mediated via the induction of p53 target genes by hnRNP K.

Materials and methods

Tissue samples, histology and immunohistochemistry (IHC). A total of 68 consecutive cases of invasive adenocarcinoma of the rectum, in patients who had undergone prior radiotherapy and/or chemotherapy, and 14 corresponding pre-therapeutic biopsies from a total of 68 patients were included in the present study (Table I). The tissue specimens were fixed in 4% buffered formaldehyde at room temperature for 24 h and subsequently embedded in paraffin. For each post-RCTx case, full histological slides were re-reviewed for the percentage of vital tumor cells to assess the tumor regression grade according to Dworak *et al* (7). For all cases, two representative regions (x10 field; 4.909 mm²) per case were selected for the creation of a tissue microarray (TMA). Immunohistochemistry was performed on a Ventana Autostainer (Ventana, Tucson, AZ, USA) following heat-induced epitope retrieval (HIER; pH 8.0; 32 min for hnRNP K and p21, and 60 min for p53, respectively) using the following antibodies: Anti-hnRNP K (cat. no. LS-C30312-50; rabbit polyclonal; 1:250, Biozol, Eching, Germany; incubation at 37°C for 24 min), anti-p53 (clone DO7; cat. no. 790-2912; mouse monoclonal; prediluted to ~0.5 µg/ml; Ventana; incubation at 37°C for 16 min) and anti-p21 (cat. no. 760-4453; mouse monoclonal; prediluted to ~4.83 µg/ml; Ventana; incubation at 37°C for 24 min). The OptiView Diaminobenzidine IHC detection kit (Ventana), which eliminates the requirement for blocking reagents by the use of HRP multimer technology, was used for detection,

following the manufacturer's protocol. The IHC staining intensities were graded as absent (0), weak (1) and strong (2) using x10 magnification on a Leica DM6000B light microscope (Leica Microsystems GmbH, Wetzlar, Germany).

Sanger sequencing. DNA from FFPE specimens was extracted with the Maxwell® 16 FFPE Tissue LEV DNA Purification kit with the use of the Maxwell® 16 AS3000 instrument (both Promega Corporation, Madison, WI, USA). Amplification of the KRAS Exon 2 polymerase chain reaction (PCR) products was performed with the following PCR primers: Forward, 5'-GTCACATTTTCATTATTTTTATTATAAGGCCTG-3' and reverse, 5'-CCTCTATTGTTGGATCATATTCGTCCAC-3'. PCR was performed with 10 µl Gene Amp™ Fast PCR Master mix (Thermo Fisher Scientific, Inc., Waltham, MA, USA), 2.8 µl each of the forward and reverse primers (1 pmol/µl), 2.8 µl nuclease-free water and 2 µl DNA (undiluted and 1:10 diluted without prior quantification), with an initial denaturation at 95°C for 10 sec, and 40 cycles of denaturation at 94°C for 10 sec and annealing at 63°C for 20 sec. The sequencing PCR was performed with an initial denaturation at 96°C for 1 min (25 cycles), at 96°C for 10 sec, 50°C for 5 sec and 60°C for 1.15 min using the BigDye® Terminator v3.1 Mix Cycle Sequencing kit (Thermo Fisher Scientific, Inc.) and the gene specific primers mentioned above. Following purification with MultiScreen®-HV plates (Merck Millipore, Darmstadt, Germany) and Sephardi G-50 (GE Healthcare Life Sciences, Chalfont, UK) the PCR products were sequenced using a 96-capillary 3730xl DNA analyzer (Thermo Fisher Scientific, Inc.).

Next-generation sequencing. In addition to KRAS mutation analysis by Sanger sequencing, samples with low tumor cell content were analyzed by more sensitive next-generation sequencing with the use of a Custom GeneRead DNASeq Panel (Qiagen GmbH, Hilden, Germany) consisting of 189 amplicons for mutation analysis of 19 cancer-related genes, (*NRAS, H3F3A, RET, KRAS, AKT1, TP53, ERBB2, H3F3B, GNA11, ALK, GNAS, CTNNB1, PIK3CA, PDGFRA, KIT, EGFR, MET, BRAF, GNAQ*), according to the manufacturer's protocol. In brief, genomic DNA was quantified and target enrichment was processed with the GeneRead DNAseq Panel PCR V2 kit (Qiagen GmbH) applying 40 ng genomic DNA quantified with a Qubit® dsDNA HS kit and a Qubit® 2.0 Fluorometer (Life Technologies; Thermo Fisher Scientific, Inc.). An initial activation step (95°C; 15 min) was followed by 25 cycles of denaturing at 95°C (15 sec) and annealing at 60°C (4 min), followed by extension at 72°C for 10 min. All purification and size selection steps were performed using Agencourt AMPure XP magnetic beads (Beckman Coulter, Inc., Brea, CA, USA). End repair, A-addition and ligation to NEXTflex-96 DNA barcodes (Bioo Scientific, Austin, TX, USA) were performed using the GeneRead DNA Library I Core kit (Qiagen GmbH). Amplification of adapter-ligated DNA was conducted using NEXTflex primers (Bioo Scientific) and the HiFi PCR Master mix (GeneRead DNA I Amp kit; Qiagen GmbH) with an initial activation step of 98°C (2 min), five cycles of denaturation at 98°C (20 sec), annealing at 60°C (30 sec) and extension at 72°C (30 sec), followed by a final extension at 72°C (10 min). Following a final purification with Agencourt AMPure XP Beads (Beckman Coulter, Inc.), the library PCR products
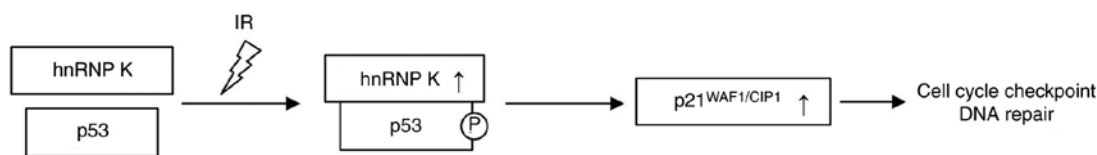
Figure 1. Schematic model of a possible role for hnRNP K as a transcriptional cofactor for p53 in the induction of p21[WAF1/CIP1] following DNA damage. hnRNP K, heterogeneous nuclear ribonucleoprotein K; IR, ionizing radiation.

were quantified, diluted, pooled and sequenced using the MiSeq™ V2 reagent kit on an MiSeq™ instrument (Illumina, Inc., San Diego, CA, USA). The data were exported as FASTQ files and analyzed via the CLC Biomedical Genomic Workbench version 3.0.1 (Qiagen GmbH).

Cell culture, cell transfection experiments and in vitro X-ray irradiation. The SW480 and Colo320 CRC cell lines were newly purchased from the Leibniz Institute DSMZ (Braunschweig, Germany). The cells were maintained in RPMI-1640 medium (Gibco, Thermo Fisher Scientific, Inc.) supplemented with 10% FCS (Boehringer Mannheim, Mannheim, Germany) under standard cell culture conditions ($37°C$, 5% CO_2). The reagents for transfection experiments included Lipofectamine 2000 transfection reagent (Invitrogen, Thermo Fisher Scientific, Inc.), Silencer® Select hnRNP K (sequence: 3'-AUAAUCAUAGGUUUCAUCGta; 5'-CGAUGAAACCUAUGAUUAUtt) and Silencer® Select negative control siRNA #1 (Thermo Fisher Scientific, Inc.). The transfected cells were harvested at 48 h or underwent treatment according to the experimental protocol. Exposure of the cells to 240 kV X-rays was performed using the YXLON Maxishot system (Hamburg, Germany) with a 3-mm beryllium filter. The dose rate rose to a plateau at 1 Gy/min at 13 mA. The absorbed dose was determined using a PTW Unidose dosimeter (PTW Freiburg GmbH, Freiburg, Germany). To guarantee equal surrounding conditions, non-irradiated SW480 and Colo320 control cells were stored under equivalent conditions at room temperature during the irradiation experiments.

PathScan stress and apoptosis signaling array. To analyze the activation of cellular stress reactions, the PathScan Stress and Apoptosis Signaling Antibody Array kit (Cell Signaling Technology, Inc., Danvers, MA, USA) was used following the manufacturer's protocol.

Western immunoblotting and protein immunoprecipitation. Immunoblotting was performed according to standard methods using the XCell Sure Lock™ Mini-Cell Electrophoresis system. For equalization of protein concentrations of whole cell lysates, a BCA Protein Assay kit was used according to the manufacturer's protocol (Thermo Fisher Scientific, Inc.) following protein extraction using radioimmunoprecipitation assay (RIPA) buffer (Cell Signaling Technology, Inc.). A total of 20 μg protein per lane was loaded on pre-cast 10% NuPAGE Bis-Tris Gels (Thermo Fisher Scientific, Inc.). Anti-GAPDH (Cell Signaling Technology, Inc.; cat. no. 3683; dilution, 1:10,000) was used as a loading control. Following protein transfer to a polyvinylidene difluoride membrane (Biozol) and blocking with 5% non-fat dry milk in PBS (Biozol), primary antibodies were incubated at $4°C$ overnight and secondary antibodies were incubated at room temperature for 60 min. The primary antibodies and concentrations were as follows: Rabbit anti-hnRNP K (Biozol; cat. no. LS-C30312-50; 1:1,000); mouse anti-phospho-p53 (Ser15; Cell Signaling Technology, Inc.; cat. no. 9286; 1:1,000); mouse anti-p53 (Cell Signaling Technology, Inc.; cat. no. 48818; 1:1,000); rabbit anti-CDKN1A (p21[WAF1/CIP1]; LifeSpan Biosciences; Biozol; cat. no. LS-B9242; 1:1,000); rabbit GAPDH (HRP-conjugated; Cell Signaling Technology, Inc.; cat. no. 3683; 1:10,000). The secondary antibodies were as follows: Goat anti-rabbit (HRP-conjugated; Dako, Glostrup, Denmark; cat. no. P044801-2; 1:10,000); rabbit anti-mouse (HRP-conjugated; Dako; P016102-2; 1:10,000). Digital image acquisition was performed using the myECL™ Imager system (Thermo Fisher Scientific, Inc.). For protein co-immunoprecipitation, the MultiMACS™ Protein A/G kit (Miltenyi Biotech, Bergisch Gladbach, Germany) was used according to the manufacturer's protocol. Briefly, the cells were lysed with RIPA buffer. Following incubation of the whole cell lysate with 2 μg of anti-p53 antibody, the antibody-p53-complex was labeled with 50 μl μMACS Protein G MicroBeads for 30 min on ice. The μMACS columns were placed in the magnetic field of the μMACS separator. The non-bound protein fraction was collected prior to washing the columns four times using the μMACS washing buffer. Subsequently, the co-immunoprecipitated proteins were eluted with pre-heated ($95°C$) 1X SDS gel loading buffer. For the analysis of non-specific protein binding, the cell lysates were incubated with microbeads only. The protein fractions were analyzed by SDS-PAGE and western blot analysis as described above.

Immunofluorescence (IF) microscopy. The IF staining was performed as previously described (13) using a rabbit monoclonal antibody targeting hnRNP K (1:250, Biozol; cat. no. LS-C30312-50)/mouse monoclonal antibody targeting Ser15-phospho-p53 (1:250, Cell Signaling Technology, Inc.; cat. no. 9286). Fluorescence-labeled secondary antibody (Alexa Fluor® 488-conjugate; donkey polyclonal anti-rabbit, 1:500; Thermo Fisher Scientific, Inc.; cat. no. A-21206) and Texas-Red-X-conjugate (goat polyclonal anti-mouse, 1:500; Thermo Fisher Scientific, Inc.; cat. no. T-6390). Primary and secondary antibodies were incubated for 1 h at room temperature in the dark. For image acquisition, a Zeiss Axioimager 2i fluorescence microscope and the ISIS fluorescence imaging system (MetaSystems, Altlussheim, Germany) were used.

Statistical analysis. Differences in IHC expression levels and between fractions of vital tumor cells (comparisons between two groups) were calculated by Student's t-test (two-tailed)
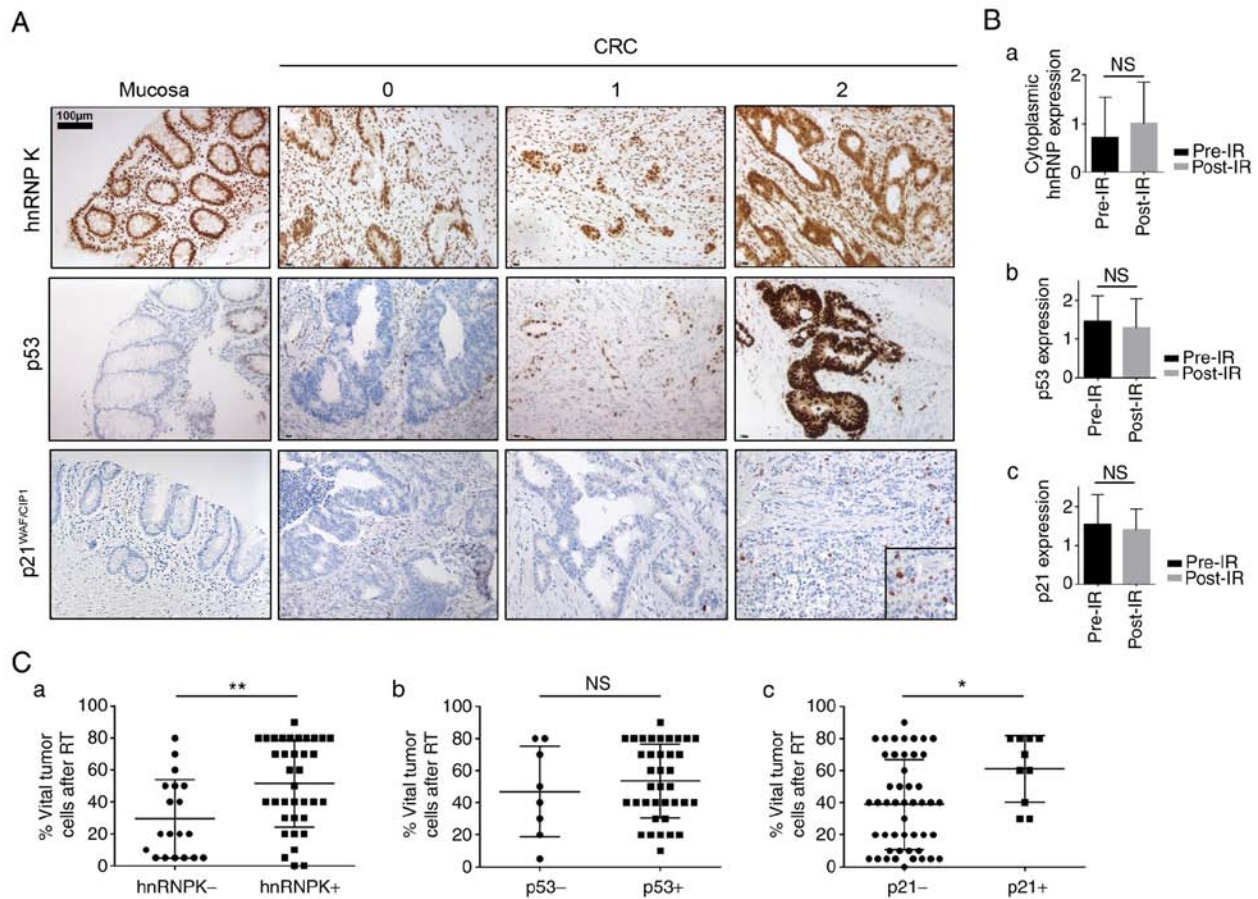
Table I. Clinicopathological data.

Clinicopathological factor	n (%)	
Patients	68 (100)	
Samples	82	
Resected specimens	68	
Pre-therapeutic biopsies	14	
Sex		
Male	49 (72)	
Female	19 (28)	
Age, years [range (median)]	32-88 (62.5)	
Therapy (n=64)		
Radiotherapy	5 (8)	
Radiotherapy + chemotherapy	59 (92)	
ypT stage (n=68)		
ypT0	10 (15)	
ypT1	5 (7)	
ypT2	17 (25)	
ypT3	33 (49)	
ypT4	3 (4)	
ypN stage (n=66)		
ypN0	42 (64)	
ypN+	24 (36)	
Dworak regression grade (n=68)		
0 (no regression)	0 (0)	
1 (predominance of tumor over fibrosis)	21 (31)	
2 (predominance of fibrosis, tumor visible)	24 (35)	
3 (fibrosis, few nests of tumor cells)	13 (19)	
4 (no visible tumor cells)	10 (15)	
Expression of hnRNP K (cytoplasmic; n=68)	Pre-therapeutic (n=14)	Post-therapeutic (n=54)
Absent (0)	12 (86)	20 (37)
Weak (1)	2 (14)	16 (30)
Strong (2)	0 (0)	18 (33)
Expression of p53 (n=59)	Pre-therapeutic (n=13)	Post-therapeutic (n=46)
Absent (0)	1 (8)	9 (19)
Weak (1)	5 (38)	16 (35)
Strong (2)	7 (54)	21 (46)
Expression of p21 (n=55)	Pre-therapeutic (n=13)	Post-therapeutic (n=43)
Absent (0)	9 (70)	35 (82)
Weak (1)	2 (15)	4 (9)
Strong (2)	2 (15)	4 (9)
KRAS codon 12/13 mutation (n=59)[a]		
Codon 12/13 mutation	9 (15)	
Codon 12/13 wild-type	50 (85)	

[a]See Table II for detailed results of the mutation analyses. hnRNP K, heterogeneous nuclear ribonucleoprotein K.

using GraphPad software (v.6; GraphPad Software, Inc., La Jolla, CA, USA). Contingency analyses (correlations between protein expression levels) were performed by χ^2 test in GraphPad. P<0.05 was considered to indicate a statistically significant difference.

Results

Clinicopathological characteristics. There were 68 patients (49 men, 19 women) and 82 tissue samples (68 resection specimens and 14 corresponding pre-therapeutic biopsies) included

Figure 2. IHC staining for hnRNP K, p53 and p21 in rectal adenocarcinoma samples. (A) representative microphotographs of absent/weak (0), moderate (1) and strong (3) staining intensities; the left panel shows expression patterns of hnRNP K, p53 and p21 in healthy colonic mucosa. Scale bar=100 μm. (B) Comparison between immunostaining intensities for (a) hnRNP K, (b) p53 and (c) p21 pre- and post-IR. (C) Fraction of vital tumor cells (tumor regression) in post-therapeutic surgical specimens with respect to expression levels of (a) hnRNP K, (b) p53 and (c) p21. *P<0.05; **P<0.01. hnRNP K, heterogeneous nuclear ribonucleoprotein K; CRC, colorectal cancer; IHC, immunohistochemistry; IR, ionizing radiation; RT, radiochemotherapy; NS, not significant.

in the present study. The detailed clinicopathological characteristics are summarized in Table I. The median patient age was 62.5 years (range, 32-88 years). In 10 patients (15%), there was complete pathological remission following neoadjuvant RCTx (ypT0, Dworak grade 4), whereas in 58 patients (85%), there were variable levels of residual tumor cells. A total of 24 patients (36%) had positive lymph nodes following therapy (ypN+) sand nine patients (15%) had *KRAS* codon 12/13 mutations. However, more detailed analysis of the data revealed that *KRAS* codon 12/13 mutations were detectable in 7/23 (30%) of pre-therapeutic tissue samples, but in only 2/36 (6%) of post-therapy resection specimens (Table II).

Expression of hnRNP K, p53 and p21 in rectal adenocarcinoma samples. The staining results for hnRNP K, p53 and p21 are summarized in Table I. Representative microphotographs of absent (0), moderate (1) and strong (2) cytoplasmic staining intensities are shown in Fig. 2A. The healthy mucosa showed immunoreactivity for hnRNP K restricted to cell nuclei, whereas p53 was expressed only in the nuclei of a subpopulation of basal crypt cells; there was no detectable p21 immunostaining in healthy colonic mucosa (left panel). Uniform cytoplasmic hnRNP K expression was only detectable in tumor tissue, and RCTx led to further upregulation of cytoplasmic hnRNP K; however, this result was not statistically significant (Fig. 2Ba;

Table II. Detailed results from *KRAS* mutation analysis.

Codon	n (%)
Samples for mutation testing	59 (100)
KRAS codon 12/13 mutation (n=59)	
Codon 12/13 mutation	9 (15)
Codon 12/13 wild-type	50 (85)
Analysis from pre-treatment material (n=23)	
Codon 12/13 mutation	7 (30)
Codon 12/13 wild-type	16 (70)
Analysis from resection specimen (n=36)	
Codon 12/13 mutation	2 (6)
Codon 12/13 wild-type	34 (94)

P=0.2669). No significant differences in the expression levels of p53 and p21 were identified when comparing post-therapeutic resection specimens to correlating pre-therapeutic biopsies (Fig. 2Bb and c; P=0.6267 and 0.4653, respectively). The fraction of vital tumor cells following RCTx was significantly higher in hnRNP K/p21-positive cases (P=0.0047 and 0.0223,
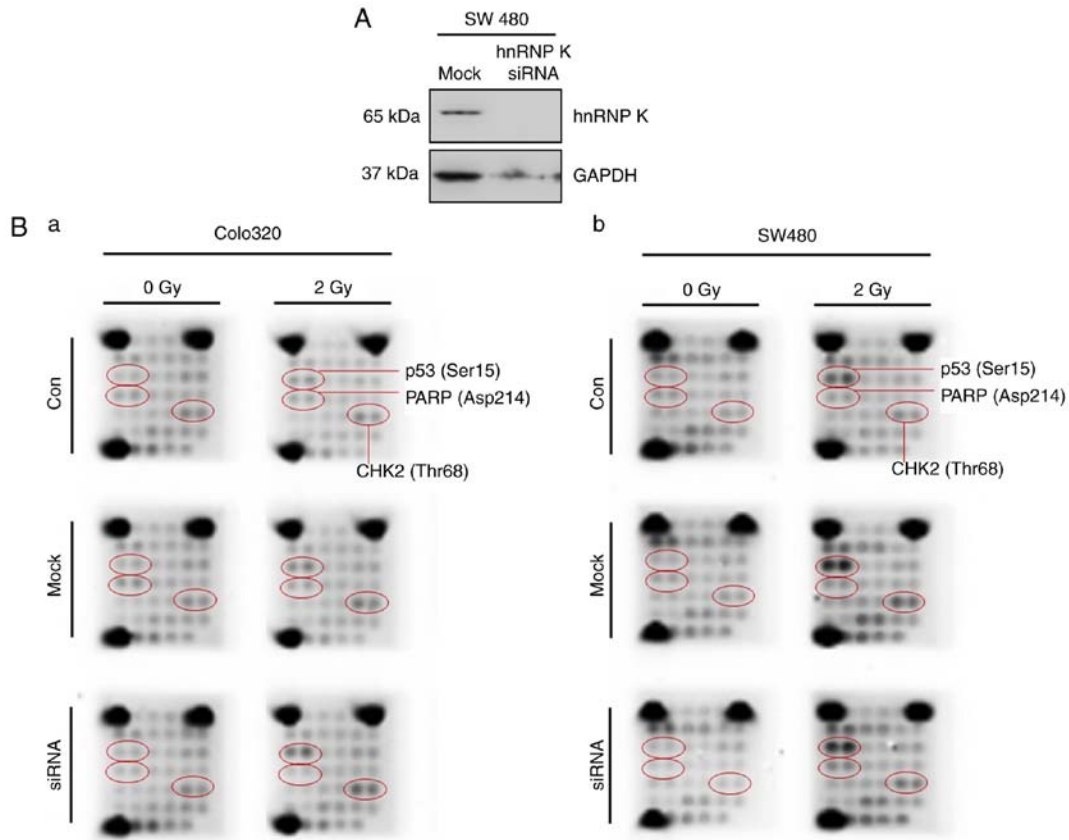
Figure 3. Analysis of intracellular signaling pathways. (A) siRNA knockdown of hnRNP K was confirmed by western immunoblotting. (B) Increases in p53 Ser15-phosphorylation, PARP cleavage and CHK2 (Thr68) phosphorylation upon ionizing radiation in (a) Colo320 and (b) SW480 cells were neither affected by mock-siRNA nor by hnRNP K-siRNA transfection. hnRNP K, heterogeneous nuclear ribonucleoprotein K; PARP, poly (ADP-ribose) polymerase; siRNA, small interfering RNA; Con, control.
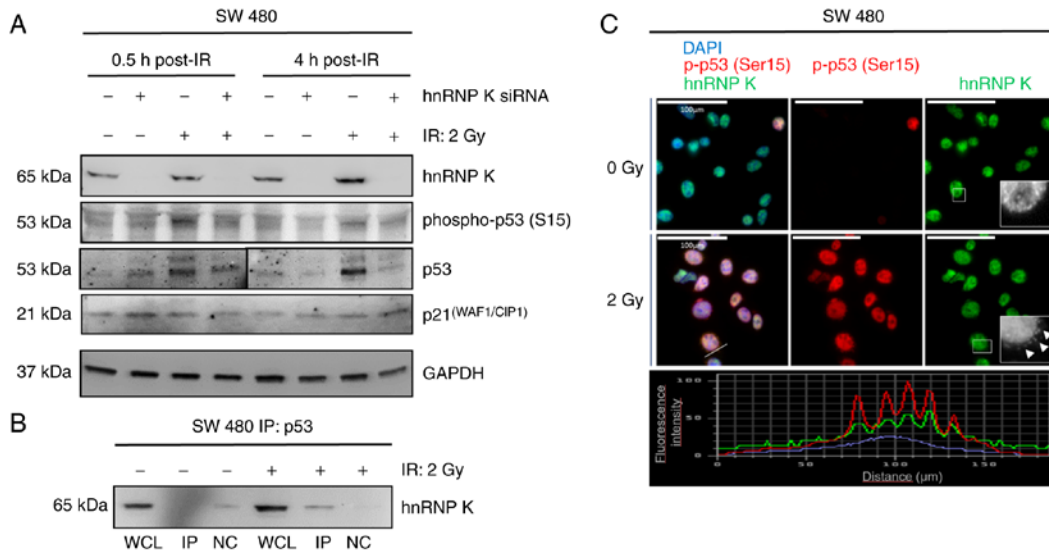

Figure 4. Protein expression levels and hnRNP K/p53 interaction upon IR. (A) Early and late effects of IR and hnRNP K on p53, p53 Ser15-phosphorylation and expression of p21 0.5 and 4 h following exposure to 2 Gy gamma-irradiation. (B) Protein co-immunoprecipitation of hnRNP K via p53 following 2 Gy gamma-irradiation. (C) p53 Ser15-phosphorylation and cytoplasmic co-localization of hnRNP K (white arrowheads) and Ser15-phosphorylated p53 in 2 Gy-irradiated SW480 cells 0.5 h following exposure to IR. Software-based measurement of fluorescence intensity confirmed the perinuclear co-localization of hnRNP K and Ser15-phosphorylated p53. hnRNP K, heterogeneous nuclear ribonucleoprotein K; IR, ionizing radiation; siRNA, small interfering RNA; p-p53, phospho-p53; WCL, whole cell lysate; IP, immunoprecipitation; NC, negative control.

respectively) and there was a significant correlation between the expression levels of hnRNP K and p53 (P=0.0125), but not p21 (P=0.2255) (Fig. 2Ca-c). No correlation was found between the fraction of vital tumor cells following RCTx and

the expression of p53 (Fig. 2Cb; P=0.4821). There was also no significant correlation between pre- or post-therapeutic hnRNP K, the expression of p53 or p21 and any clinicopathological characteristic (age, sex, ypT/N stage or *KRAS* mutation status) or between hnRNP K/p21 and p53/p21 staining intensities (P>0.05; data not shown).

PathScan intracellular signaling array upon IR and hnRNP K siRNA knockdown in vitro. To assess the effect of IR on tyrosine kinase signaling and the role of hnRNP K in the radioresistance of human CRC cells *in vitro*, Colo320 and SW480 cells were subjected to 2 Gy gamma-irradiation. Successful siRNA knockdown of hnRNP K was confirmed by western immunoblotting compared with mock-transfected cells (Fig. 3A). In the untreated Colo320 cells, IR led to a marginal increase in p53 phosphorylation (Ser15) and a marginal increase in poly (ADP-ribose) polymerase (PARP) cleavage and CHK2 (Thr68) phosphorylation (Fig. 3Ba). However, these alterations were neither affected by mock-siRNA nor by hnRNP K-siRNA transfection. There was marked Ser15 phosphorylation in response to IR in SW480 cells, however, this effect was not altered by hnRNP K siRNA knockdown (Fig. 3Bb). Only a marginal increase was found in PARP cleavage and CHK2 (Thr68) phosphorylation in response to IR.

Effect of hnRNP K siRNA knockdown on the expression of p53, p53 Ser15-phosphorylation, p53/hnRNP K interaction and expression of p21 in vitro. To assess early and late effects of IR and hnRNP K on p53 phosphorylation and the expression level of p21, western immunoblotting was performed for hnRNP K, p53, phospho-p53 (Ser15), and p21 in the mock-transfected and hnRNP K siRNA-transfected cells 0.5 and 4 h following exposure to 2 Gy gamma-irradiation (Fig. 4A). Successful siRNA-knockdown was again shown through western immunoblotting for hnRNP K. An increase in p53 Ser15-phosphorylation was detected 0.5 h and, to a lesser extent, 4 h post-IR. This change was mirrored by an increase in the expression of p53, however, these effects were eliminated by siRNA knockdown of hnRNP K at 0.5 and 4 h following IR. p53 Ser15-phosphorylation remained detectable upon hnRNP K knockdown, and no changes in the expression of p21were observed in response to IR in the presence or absence of hnRNP K. The co-immunoprecipitation experiments verified enhanced hnRNP K/p53 complex formation upon 2 Gy gamma-irradiation (Fig. 4B), and immunofluorescence microscopy confirmed the enhanced p53 Ser15-phosphorylation and cytoplasmic co-localization of hnRNP K and Ser-15 phosphorylated p53 in the 2 Gy-irradiated SW480 cells 0.5 h following exposure to IR (Fig. 4C).

Discussion

hnRNP K is upregulated in several malignancies and is involved in the regulation of transcription, mRNA maturation and translation (10,12-14). The protein has also been shown to be a key element of the DNA damage response pathway through interaction with p53 and induction of p53 target genes, including p21, as a transcriptional cofactor for p53 (16,18). In the present study, the aim was to evaluate whether hnRNP K

is involved in the radioresistance of rectal adenocarcinomas and, if this is the case, to elucidate the molecular mechanisms underlying hnRNP K-mediated resistance to RCTx. The sample cohort comprised 68 patients with a median age of 62.5 years, representing the typical age group for (colo) rectal carcinoma, with a preponderance of males (1). There was complete tumor regression upon neoadjuvant therapy (ypT0; complete pathological remission, Dworak grade 4) in 15% of patients, reflecting data from literature (6). *KRAS* codon 12/13 mutations were only detected in 15% of patients. The literature suggests that a proportion of 30-52% of CRCs harbor mutations in the *RAS* oncogene, depending on which *RAS* isoforms (*KRAS* or *NRAS*) and hotspots (codon 12/13, 59, 61, 117 and 146) are taken into account (21,22). A closer look at the results of the present study revealed that mutation analyses in pre-therapeutic tissue resulted in 30% *KRAS*-mutant tumors, which was in line with published data (21), whereas analyses in post-therapeutic specimens yielded only 6% mutation-positive tumors. This may be due to the fact that, in certain specimens, a good response to neoadjuvant therapy led to extensive scarring with minimal residual tumor cells, which led to the diagnostic limit for reliable detection of *RAS* mutation not being reached in these cases. In the present study, Sanger and next-generation sequencing were used for *KRAS* codon 12/13 mutation analyses. Sanger sequencing has a reported limit of detection of 10-20% allele frequency, whereas next-generation sequencing can detect mutations down to an allele frequency of 0.2% depending on the DNA quality of the FFPE specimens (23,24). However, in certain ypT1/Dworak 3 tumors, the actual mutated allele frequency may have been below that diagnostic threshold. Together with the limitation that only *KRAS* codons 12 and 13 mutations were analyzed, the results have to be interpreted with caution regarding the impact of *RAS* mutations, and the limitations may explain why it was not possible to verify the association between *RAS* mutations and radioresistance that has been previously reported (25,26).

No significant differences were observed between pre- and post-therapeutic levels of hnRNP K, p53 or p21 when comparing pre-therapeutic biopsies to post-therapeutic resection specimens. For hnRNP K, this observation is in line with our previous findings from malignant melanoma and from CRC, where IR induced a rapid, but temporal increase in the expression of hnRNP K (13,15). High expression levels of hnRNP K and p21 in the resection specimens correlated with poor response to prior RCTx, supporting a role for these proteins in radioresistance, and between expression levels of hnRNP K and p53. As IR-induced upregulation of p53 in intestinal epithelium has been previously described, and the hnRNP K/p53 interaction is a key element in the cellular response to IR in U2OS osteosarcoma cells, this result suggests a possible role for the interaction of hnRNP K and p53 in radioresistance of rectal adenocarcinoma, which may be mediated via p21 in CRC (16,27).

To elucidate the molecular mechanisms underlying hnRNP K-mediated radioresistance, the present study used an *in vitro* irradiation model using SW480 and Colo320 CRC cell lines. In line with published data, PathScan intracellular signaling array revealed the increased phosphorylation of p53 Ser15, PARP cleavage and phosphorylation of CHK2 (Thr68) (28-30). However, these effects were not

affected by the siRNA-mediated knockdown of hnRNP K, and thus appeared to occur independently of the presence of hnRNP K. This result is supported by data from Moumen *et al* (16), having previously shown IR-induced p53 Ser15-phosphorylation in hnRNP K-depleted cells. The SW480 line was used for further hnRNP K knockdown experiments due to its individual molecular profile. This cell line harbors two p53 point mutations that are frequently observed in CRC (Arg273His/Pro309Ser), however, p53 still binds its consensus DNA sequences with wild-type affinity and constitutively activates p21 in these cells (19,31). In addition, SW480 cells carry a *KRAS* G12V mutation, and our previous study identified hnRNP K to be a key factor in RAS-mediated radioresistance in CRC (15). Western immunoblotting of cell lysates was performed, and it was found that, in line with the results from PathScan, radiation had increased p53 Ser15-phosphorylation and the expression of p53 at 0.5 and 4 h post-IR. The marginal decrease in Ser15-phosphorylation following transfection with siRNA targeting hnRNP K may be due to the observed downregulation of the protein level of p53 upon hnRNP K knockdown; this is supported by the correlation between the expression of hnRNP K and p53 found in post-radiation patient samples. There were no detectable changes in expression levels of p21 upon IR. However, 2 Gy irradiation induced hnRNP K/p53 complex formation, as demonstrated by protein co-immunoprecipitation of hnRNP K via p53 and cytoplasmic co-localization of hnRNP K and Ser15-phosphorylated p53 in immunofluorescence microscopy. These results confirmed that, although IR upregulated hnRNP K and p53 and enhanced the interaction of hnRNP K with (phospho-)p53 in the cytoplasm, p53 Ser15-phosphorylation occurred independently from the presence of hnRNP K. There were no changes in the expression of p21 in response to IR, and basal levels of p21 remained detectable following hnRNP K siRNA knockdown.

Taken together, the results of the present study add to the evidence that hnRNP K is important in the radioresistance of CRC, comparable to our previous results and findings in other tumors (13,15). The radioprotective effect of hnRNP K appeared to be independent of the hnRNP K-mediated caspase inhibition that has been described previously (32), as the knockdown of hnRNP K had no effect on PARP cleavage in the *in vitro* irradiation model. The effect may instead be mediated via cytoplasmic interaction of hnRNP K with phosphorylated p53, as the expression levels of the two proteins in post-therapy tissue specimens were significantly correlated, and gamma-irradiation enhanced cytoplasmic hnRNP K/p53 complex formation and hnRNP K/phospho-p53 co-localization *in vitro*. However, it is unlikely to be mediated via the induction of p21 downstream in the p53 pathway, which is known to be activated upon IR in human osteosarcoma (U2OS) cells (18). Instead, as hnRNP K has been shown to regulate the maturation and translation of multiple target mRNAs relevant to oncogenic transformation and proliferation, it may be that the hnRNP K/(phospho-)p53 interaction has an impact on hnRNP K-mediated mRNA processing (11,34). For example, hnRNP K binds to a CU-rich element in thymidine phosphorylase (TP) mRNA, resulting in the upregulation of TP and resistance to apoptosis in nasopharyngeal carcinoma (34). In addition, hnRNP Q has been shown to bind

to the 5'-untranslated region of mouse p53 mRNA and thus regulates the translation of p53, which suggests the possibility of a similar regulatory circuit involving hnRNP K and p53 in CRC cells (35). Further investigations are required to clarify whether the IR-induced hnRNP K/p53 interaction in the cytoplasm modulates the binding of hnRNP K to its mRNA targets, and whether hnRNP K is involved in regulating the protein expression of p53. Elucidating these mechanisms may ultimately assist in the identification of radiosensitizing compounds to improve biological response to radiotherapy applied to rectal adenocarcinomas in a neoadjuvant or palliative setting.

In conclusion, the results of the present study support a radioprotective role for hnRNP K in rectal adenocarcinoma, which may be mediated through its interaction with p53. However, this effect appears to be independent of the hnRNP K/p53-induced upregulation of p21.

Availability of data and materials

All data generated or analyzed in the present study are included in this published article.

Authors' contributions

KSteinestel and WD performed (immuno-)histological analyses; WD, KStock and JS performed *KRAS* mutation analyses. SE performed *in vitro* analyses. KSteinestel, EW, MP, SH and SE conceived the study, were involved in its design and coordination, and assisted in drafting the manuscript. All authors read and approved the final manuscript.

Ethics approval and consent to participate

All tissue samples were collected for histologic examination and diagnostic purposes and anonymized for use in the study in accordance with The Code of Ethics of the World Medical Association (Declaration of Helsinki). Informed consent was therefore not required. The study received institutional review board approval from the Ethics Committee of the University of Münster (no. 2015-628-f-S).

Patient consent for publication

Not applicable.

Competing interests

The authors declare that they have no competing interests.

References

1. Siegel R, DeSantis C and Jemal A: Colorectal cancer statistics, 2014. CA Cancer J Clin 64: 104-117, 2014.
2. Wei EK, Giovannucci E, Wu K, Rosner B, Fuchs CS, Willett WC and Colditz GA: Comparison of risk factors for colon and rectal cancer. Int J Cancer 108: 433-442, 2004.
3. Kapiteijn E, Marijnen CA, Nagtegaal ID, Putter H, Steup WH, Wiggers T, Rutten HJ, Pahlman L, Glimelius B, van Krieken JHJ, et al: Preoperative radiotherapy combined with total mesorectal excision for resectable rectal cancer. N Engl J Med 345: 638-646, 2001.
4. Cammà C, Giunta M, Fiorica F, Pagliaro L, Craxì A and Cottone M: Preoperative radiotherapy for resectable rectal cancer: A meta-analysis. JAMA 284: 1008-1015, 2000.
5. Schmiegel W, Pox C, Reinacher-Schick A, Adler G, Fleig W, Fçlsch U, Frühmorgen P, Graeven U, Hohenberger W, Holstege A, et al: S3-Leitlinie, Kolorektales Karzinom Ergebnisse evidenzbasierter Konsensuskonferenzen am 6./7. Februar 2004 und am 8./9. Juni 2007 (für die Themenkomplexe IV, VI und VII). Z Gastroenterol 46: 1-73, 2008 (In German).
6. Maas M, Nelemans PJ, Valentini V, Das P, Rödel C, Kuo L-J, Calvo FA, García-Aguilar J, Glynne-Jones R and Haustermans K: Long-term outcome in patients with a pathological complete response after chemoradiation for rectal cancer: A pooled analysis of individual patient data. Lancet Oncol. 11: 835-844, 2010.
7. Dworak O, Keilholz L and Hoffmann A: Pathological features of rectal cancer after preoperative radiochemotherapy. Int J colorectal dis 12: 19-23, 1997.
8. Becker K, Mueller JD, Schulmacher C, Ott K, Fink U, Busch R, Böttcher K, Siewert JR and Höfler H: Histomorphology and grading of regression in gastric carcinoma treated with neoadjuvant chemotherapy. Cancer 98: 1521-1530, 2003.
9. Wittekind C and Tannapfel A: Regressionsgrading des präoperativ-radiochemotherapierten rektumkarzinoms. Der Pathologe 24: 61-65, 2003 (In German).
10. Bomsztyk K, Denisenko O and Ostrowski J: hnRNP K: One protein multiple processes. Bioessays 26: 629-638, 2004.
11. Ostareck-Lederer A, Ostareck DH, Cans C, Neubauer G, Bomsztyk K, Superti-Furga G and Hentze MW: c-Src-mediated phosphorylation of hnRNP K drives translational activation of specifically silenced mRNAs. Mol Cell Biol 22: 4535-4543, 2002.
12. Carpenter B, McKay M, Dundas S, Lawrie L, Telfer C and Murray G: Heterogeneous nuclear ribonucleoprotein K is over expressed, aberrantly localised and is associated with poor prognosis in colorectal cancer. Br J Cancer 95: 921-927, 2006.
13. Eder S, Lamkowski A, Priller M, Port M and Steinestel K: Radiosensitization and downregulation of heterogeneous nuclear ribonucleoprotein K (hnRNP K) upon inhibition of mitogen/extracellular signal-regulated kinase (MEK) in malignant melanoma cells. Oncotarget 6: 17178-17191, 2015.
14. Barboro P, Ferrari N and Balbi C: Emerging roles of heterogeneous nuclear ribonucleoprotein K (hnRNP K) in cancer progression. Cancer Lett 352: 152-159, 2014.
15. Eder S, Arndt A, Lamkowski A, Daskalaki W, Rump A, Priller M, Genze F, Wardelmann E, Port M, and Steinestel K: Baseline MAPK signaling activity confers intrinsic radioresistance to KRAS-mutant colorectal carcinoma cells by rapid upregulation of heterogeneous nuclear ribonucleoprotein K (hnRNP K). Cancer Lett 385: 160-167, 2017.
16. Moumen A, Masterson P, O'Connor MJ and Jackson SP: hnRNP K: An HDM2 target and transcriptional coactivator of p53 in response to DNA damage. Cell 123: 1065-1078, 2005.
17. Enge M, Bao W, Hedström E, Jackson SP, Moumen A and Selivanova G: MDM2-dependent downregulation of p21 and hnRNP K provides a switch between apoptosis and growth arrest induced by pharmacologically activated p53. Cancer cell 15: 171-183, 2009.
18. Moumen A, Magill C, Dry KL and Jackson SP: ATM-dependent phosphorylation of heterogeneous nuclear ribonucleoprotein K promotes p53 transcriptional activation in response to DNA damage. Cell Cycle 12: 698-704, 2013.
19. Shimura T, Kakuda S, Ochiai Y, Nakagawa H, Kuwahara Y, Takai Y, Kobayashi J, Komatsu K and Fukumoto M: Acquired radioresistance of human tumor cells by DNA-PK/AKT/GSK3β-mediated cyclin D1 overexpression. Oncogene 29: 4826-4837, 2010.
20. Bae I, Fan S, Bhatia K, Kohn KW, Fornace AJ and O'Connor PM: Relationships between G_1 arrest and stability of the p53 and $p21^{Cip1/Waf1}$ proteins following γ-irradiation of human lymphoma cells. Cancer Res 55: 2387-2393, 1995.
21. Douillard JY, Oliner KS, Siena S, Tabernero J, Burkes R, Barugel M, Humblet Y, Bodoky G, Cunningham D and Jassem J: Panitumumab-FOLFOX4 treatment and RAS mutations in colorectal cancer. N Engl J Med 369: 1023-1034, 2013.
22. Fernández-Medarde A and Santos E: Ras in cancer and developmental diseases. Genes Cancer 2: 344-358, 2011.
23. Moskalev EA, Stöhr R, Rieker R, Hebele S, Fuchs F, Sirbu H, Mastitsky SE, Boltze C, König H and Agaimy A: Increased detection rates of EGFR and KRAS mutations in NSCLC specimens with low tumour cell content by 454 deep sequencing. Virchows Arch 462: 409-419, 2013.
24. Tsiatis AC, Norris-Kirby A, Rich RG, Hafez MJ, Gocke CD, Eshleman JR and Murphy KM: Comparison of sanger sequencing, pyrosequencing, and melting curve analysis for the detection of KRAS mutations: diagnostic and clinical implications. J Mol Diagn 12: 425-432, 2010.
25. Wang M, Kern AM, Hulskotter M, Greninger P, Singh A, Pan Y, Chowdhury D, Krause M, Baumann M, Benes CH, et al: EGFR-mediated chromatin condensation protects KRAS-mutant cancer cells against ionizing radiation. Cancer Res 74: 2825-2834, 2014.
26. Gupta AK, Bakanauskas VJ, Cerniglia GJ, Cheng Y, Bernhard EJ, Muschel RJ and McKenna WG: The Ras radiation resistance pathway. Cancer Res 61: 4278-4282, 2010.
27. Qiu W, Leibowitz B, Zhang L and Yu J: Growth factors protect intestinal stem cells from radiation-induced apoptosis by suppressing PUMA through the PI3K/AKT/p53 axis. Oncogene 29: 1622-1632, 2010.
28. Canman CE, Lim DS, Cimprich KA, Taya Y, Tamai K, Sakaguchi K, Appella E, Kastan MB and Siliciano JD: Activation of the ATM kinase by ionizing radiation and phosphorylation of p53. Science 281: 1677-1679, 1998.
29. Ward IM, Wu X and Chen J: Threonine 68 of Chk2 is phosphorylated at sites of DNA strand breaks. J Biol Chem 276: 47755-47758, 2001.
30. Chinnaiyan P, Vallabhaneni G, Armstrong E, Huang SM and Harari PM: Modulation of radiation response by histone deacetylase inhibition. Int J Radiat Oncol Biol Phys 62: 223-229, 2005.
31. Rochette PJ, Bastien N, Lavoie J, Guérin SL and Drouin R: SW480, a p53 double-mutant cell line retains proficiency for some p53 functions. J Mol Biol 352: 44-57, 2005.
32. Xiao Z, Ko HL, Goh EH, Wang B and Ren EC: hnRNP K suppresses apoptosis independent of p53 status by maintaining high levels of endogenous caspase inhibitors. Carcinogenesis 34: 1458-1467, 2013.
33. Evans JR, Mitchell SA, Spriggs KA, Ostrowski J, Bomsztyk K, Ostarek D and Willis AE: Members of the poly (rC) binding protein family stimulate the activity of the c-myc internal ribosome entry segment in vitro and in vivo. Oncogene 22: 8012-8020, 2003.
34. Chen LC, Liu HP, Li HP, Hsueh C, Yu JS, Liang CL and Chang YS: Thymidine phosphorylase mRNA stability and protein levels are increased through ERK-mediated cytoplasmic accumulation of hnRNP K in nasopharyngeal carcinoma cells. Oncogene 28: 1904-1915, 2009.
35. Kim D, Kim W, Lee K, Kim S, Lee H, Kim H, Jung Y, Choi J and Kim K: hnRNP Q regulates translation of p53 in normal and stress conditions. Cell Death Differ 20: 226-234, 2013.